Geosci. Model Dev. Discuss., doi:10.5194/gmd-2016-40, 2016
Manuscript under review for journal Geosci. Model Dev.
Published: 7 March 2016

Geoscientific Model Development Discussions

C-IFS-CB05-BASCOE: Stratospheric Chemistry in the Integrated Forecasting System of ECMWF

Vincent Huijnen[1], Johannes Flemming[2], Simon Chabrillat[3], Quentin Errera[3], Yves Christophe[3], Anne-Marlene Blechschmidt[4], Andreas Richter[4], Henk Eskes[1]

[1]Royal Netherlands Meteorological Institute, De Bilt, The Netherlands
[2]European Centre for Medium-Range Weather Forecasts, Reading, UK
[3]Belgian Institute for Space Aeronomy (BIRA-IASB), Brussels, Belgium
[4]Institute of Environmental Physics, University of Bremen, Germany

Correspondence to: Vincent Huijnen (Huijnen@knmi.nl)

Abstract. We present a model description and benchmark evaluation of an extension of the tropospheric chemistry module in the Integrated Forecasting System (IFS) of the European Centre for Medium-Range Weather Forecasts (ECMWF) with stratospheric chemistry, referred to as C-IFS-CB05-BASCOE (for brevity here referred to as C-IFS-TS). The stratospheric chemistry originates from the one used in the Belgian Assimilation System for Chemical ObsErvations (BASCOE), and is here combined with the modified CB05 chemistry module for the troposphere as currently used operationally in the Copernicus Atmosphere Monitoring Service (CAMS). In our approach either the tropospheric or stratospheric chemistry module is applied depending on the altitude of each individual grid box with respect to the tropopause. An evaluation of a 1.5 year long C-IFS-TS simulation indicates good performance of the system in terms of stratospheric ozone, nitrogen dioxide as well as other reactive tracers in comparison to various satellite retrieval products. This marks a first step towards a chemistry module within IFS that encompasses both tropospheric and stratospheric composition.

1 Introduction

Existing earth observation systems in combination with global circulation models (GCMs) help to provide a better understanding of the Earth's atmospheric composition and changes therein (Hollingsworth et al., 2008). For the troposphere, hemispheric transport and chemical conversion of atmospheric composition influences regional air quality (Pausata et al., 2012; Im et al., 2015, Marécal et al., 2015). Also analyses and forecasts of stratospheric ozone directly impact the forecast capabilities of surface solar irradiance (Qu et al., 2014). Stratospheric ozone further affects the chemical composition in the troposphere because of stratosphere-troposphere transport of ozone (Stevenson et al., 2006, Gaudel et al., 2015), and its radiative properties influencing the tropospheric photolysis rates. Beyond such direct implications a comprehensive description of stratospheric composition allows a more complete understanding of processes taking place in the stratosphere, ranging from tracking the ozone hole (Lefever et al., 2015) and understanding the concentrations of ozone depleting substances (Chipperfield et al., 2015), to the assessment of dynamical effects such as the Quasi-Biennial Oscillation (QBO,

Geosci. Model Dev. Discuss., doi:10.5194/gmd-2016-40, 2016
Manuscript under review for journal Geosci. Model Dev.
Published: 7 March 2016

Baldwin et al., 2001), and from implications of sudden stratospheric warmings on circulation patterns (Manney et al., 2015) to general radiative feedbacks of ozone, water vapor and CO_2 on weather and climate (Solomon et al., 2010).

These aspects have long been studied in the framework of Chemistry Transport Models (CTMs) and, more recently, in GCMs, see, e.g., the SPARC Chemistry-Climate Model Validation Activity (CCMVal, 2010). In GCMs the role of stratospheric ozone chemistry on the tropospheric climate can explicitly be studied (e.g. Scaife et al., 2011). But also meteorological models can benefit from having a good representation of the stratospheric composition and its variability, considering the radiative effects and the resulting impact on stratospheric as well as tropospheric temperatures (Monge-Sanz et al., 2013), which becomes relevant for tropospheric forecast skills on long-range to seasonal time scales (Maycock et al., 2011).

Within a series of MACC (Monitoring Atmospheric Composition and Climate) European research projects a global forecast and assimilation system has been built, which is the core for the global system of the Copernicus Atmosphere Monitoring Service, (CAMS, http://atmosphere.copernicus.eu). In CAMS, forecasts of atmospheric composition are carried out (Flemming et al., 2015, Morcrette et al., 2009, Engelen et al. 2009), which benefit from assimilation of satellite retrievals (Inness et al., 2015, Benedetti et al., 2009), to improve the initial conditions for composition fields in terms of reactive gases, aerosols and greenhouse gases. Here a tropospheric chemistry scheme has been embedded in ECMWF's Integrated Forecast System, referred to as Composition-IFS (C-IFS, Flemming et al., 2015). Even though the current operational version of C-IFS based on the Carbon Bond chemistry scheme (CB05) provides good model capability on tropospheric composition (Eskes et al., 2015), the stratosphere is only realistically constrained in terms of ozone. This is because so far the model ozone is based on a linear scheme (Cariolle and Tyssèdre, 2007) which is suitable owing to the data-assimilation capabilities of C-IFS of both total column and profile satellite retrievals (Flemming et al., 2011; Inness et al., 2015; Lefever et al., 2015).

Also it is recognized that the applicability of radiation feedbacks of tracer fields, such as ozone and water vapor, as produced through CH_4 oxidation, are hampered by schemes that are based on linearizations (Cariolle and Morcrette, 2006; de Grandpré et al., 2009), due to their intrinsic dependencies to climatologies which are used to construct such schemes and hence may behave poorly in anomalous situations. Having full stratospheric chemistry available in the IFS therefore would not only allow to study a wider range of atmospheric composition processes, but also a more independent assessment of radiation feedbacks on temperature, hence providing the potential for improvements in stratospheric and tropospheric meteorology. These considerations drive the need for extension of C-IFS with a module for stratospheric chemistry. For this we use the chemistry scheme from the Belgian Assimilation System for Chemical ObsErvations (BASCOE), Errera et al. (2008), which was developed to assimilate satellite observations of stratospheric composition.

BASCOE is based on a Chemistry Transport Model (CTM) of the stratosphere which is used to investigate stratospheric photochemistry (Theys et al., 2010; Muncaster et al., 2012). The assimilation system uses the 4D-VAR algorithm (Talagrand and Courtier, 1987) to produce reanalyses of stratospheric composition (Viscardy et al., 2010) which compare favourably well with similar systems (Geer et al., 2006; Thornton et al., 2009) and facilitate detailed studies of transport processes in the stratosphere (Lahoz et al., 2011). The photochemistry module from the BASCOE-CTM was implemented into the Canadian

Geosci. Model Dev. Discuss., doi:10.5194/gmd-2016-40, 2016
Manuscript under review for journal Geosci. Model Dev.
Published: 7 March 2016

assimilation system GEM, demonstrating the potential of a coupled chemical-dynamical assimilation system for stratospheric studies (de Grandpré et al., 2009; Robichaud et al., 2010). BASCOE has been used and evaluated within the framework of MACC as an independent system for the provision of Near Real-Time analyses of stratospheric ozone and for the validation of the corresponding product by the main assimilation system (Lefever et al., 2015; Eskes et al., 2015).

We have developed a strategy for merging the CB05 tropospheric chemistry scheme and the stratospheric chemistry scheme used in BASCOE within C-IFS. An assessment of the two chemistry schemes showed that there is only partial overlap in tracers and reactions that are essential in both regimes. For instance, 15 out of the full list of 99 tracers need to be treated in the chemical mechanisms for both troposphere and stratosphere. Also the modelling of the photolysis rates and heterogeneous reactions have been optimized for application in troposphere and stratosphere separately. Therefore we did not aim at a full integration of the chemistry schemes, but rather choose a flexible setup where -within a single framework- either the tropospheric or stratospheric chemistry modules are addressed.

In this paper we describe our modeling strategy and provide a benchmark evaluation of the merged C-IFS-TS system with focus on the stratospheric composition. The paper is organized as follows: In Sect 2 the chemistry modules for the stratosphere are described and the merging with the tropospheric scheme is explained.. Section 3 provides details on the setup of the model runs, and the observational data used for the model evaluation. Section 4 provides a basic model evaluation of the system. We finalize this manuscript with conclusions and an outlook for further work.

2. Atmospheric chemistry in C-IFS

For general aspects related to chemistry modeling in the C-IFS the reader is referred to Flemming et al. (2015). The meteorological model in the current version of C-IFS is based on IFS cycle 41r1 (http://www.ecmwf.int/en/forecasts/documentation-and-support/changes-ecmwf-model). The advection is simulated with a three-dimensional semi-Lagrangian advection scheme, which applies a quasi-monotonic cubic interpolation of the departure values.

In the following two subsections we describe the C-IFS modules for the stratospheric (referred to as BASCOE) and tropospheric (CB05) chemistry parameterizations, continued by a section describing the merging procedure of these two modules to form the C-IFS-TS system. The full list of trace gases is given in Table A1 in the Appendix, including the domains where they are actively treated within the chemistry.

2.1 Stratospheric chemistry

From the BASCOE system (Errera et al., 2008) the chemical scheme and the parameterization for Polar Stratospheric Clouds (PSC) has been implemented in the C-IFS. The BASCOE chemical scheme used here is labelled “sb14a”. It includes 58 species interacting through 142 gas-phase, 9 heterogeneous and 52 photolytic reactions. This chemical scheme merges the reaction lists developed by Errera and Fonteyn (2001) to produce short-term analyses, with the list included in the

Geosci. Model Dev. Discuss., doi:10.5194/gmd-2016-40, 2016
Manuscript under review for journal Geosci. Model Dev.
Published: 7 March 2016

SOCRATES 2-D model for long-term studies of the middle atmosphere (Brasseur et al., 2000; Chabrillat and Fonteyn, 2003). The resulting list of species (see Table A1) includes all the ozone-depleting substances and greenhouse gases necessary for multi-decadal simulations of the couplings between dynamics and chemistry in the stratosphere, as well as the reservoir and short-lived species necessary for a complete description of stratospheric ozone photochemistry.

Gas-phase and heterogeneous reaction rates are taken from JPL evaluation 17 (Sander et al., 2011) and JPL evaluation 13 (Sander et al., 2000), respectively. Lookup tables of photolysis rates were computed offline by the TUV package (Madronich and Flocke, 1999) as a function of log-pressure altitude, ozone overhead column and solar zenith angle. The photolysis tables used in chemical scheme sb14a are based on absorption cross-sections from JPL evaluation 15 (Sander et al., 2006). The kinetic rates for heterogeneous chemistry are determined by the parameterization of Fonteyn and Larsen (1996), using classical expressions for the uptake coefficients on sulfate aerosols (Hanson and Ravishankara, 1994) and on Polar Stratospheric Clouds (PSCs) (Sander et al., 2000).

The surface area density of stratospheric aerosols uses the same climatology as Daerden et al. (2007), while the surface area densities of PSCs is computed from a simple cold-point parameterization. Ice PSCs are presumed to exist at any grid point in the winter/spring polar regions where the temperature is colder than 186 K, and Nitric Acid Tri-hydrate (NAT) PSCs where the temperature is colder than 194 K. The surface area density is set to 10^{-6} cm^2/cm^3 for ice PSCs and 10^{-7} cm^2/cm^3 for NAT PSCs. The sedimentation of PSC particles causes denitrification and dehydration. This process is approximated by an exponential decay of HNO_3 with a characteristic time-scale of 100 days for gridpoints where NAT particles are supposed to exist, and an exponential decay of HNO_3 and H_2O with a characteristic time-scale of 9 days for gridpoints where ice particles are supposed to exist.

Mass mixing ratios for N_2O, CO_2 and a selection of anthropogenic and organic halogenic trace gases are constrained at the surface by a global mean constant value, Table 1. Assuming that trace gases are well mixed in the troposphere, this essentially serves as lower boundary conditions for the stratospheric chemistry.

2.2 Tropospheric chemistry

The tropospheric chemistry in the C-IFS is based on the CB05 mechanism (Yarwood et al., 2005). It adopts a lumping approach for organic species by defining a separate tracer species for specific types of functional groups. The scheme has been modified and extended to include an explicit treatment of C1 to C3 species as described in Williams et al., (2013), and SO_2, di-methyl sulphide (DMS), methyl sulphonic acid (MSA) and ammonia (NH3) (Huijnen et al., 2010). A coupling to the MACC aerosol model is available (Huijnen et al., 2014), but not switched on for this study. The reaction rates follow the recommendations given in either Sander et al. (2011) or Atkinson et al. (2006). The modified band approach (MBA), which is adopted for the computation of photolysis rates (Williams et al., 2012), uses 7 absorption bands across the spectral range 202 − 695 nm. At instances of large solar zenith angles (71-85°) a different set of band intervals is used. In the MBA the radiative transfer calculation using the absorption and scattering components introduced by gases, aerosols and clouds is computed on-line for each of the predefined band intervals. The complete chemical mechanism as applied for the

Geosci. Model Dev. Discuss., doi:10.5194/gmd-2016-40, 2016
Manuscript under review for journal Geosci. Model Dev.
Published: 7 March 2016

troposphere is extensively documented in Flemming et al. (2015). A specification of the emissions and deposition of tropospheric reactive trace gases is provided as well.

2.3 Merging procedure for the tropospheric and stratospheric chemistry

In this section we describe the strategy for merging the chemistry modules for the troposphere and stratosphere to form the C-IFS-TS system. Key chemical cycles differ between troposphere and stratosphere, hence requiring different parameterizations. For example, the oxidation of non-methane hydrocarbons (NMHC's) is essentially taking place in the troposphere and represents an important driver for tropospheric O_3 production. The chemical evolution of PAN and organic nitrate can be neglected in the stratosphere. On the other hand, N_2O and CFC's are essentially chemically inactive in the troposphere and will only photolyse by UV radiation in the stratosphere. Therefore, only the transport of those trace gases needs to be accounted for in the troposphere. Associated chemistry involving single atom radicals, such as N, O, Br, Cl, can only be produced in the stratosphere. Also the parameterization of the photolysis rates leads to different requirements for the troposphere and stratosphere, as will be discussed in the next subsection. Finally the numerical solver of the chemical mechanism contributes substantially to the total costs of the model run in terms of run-time, depending on the size of the reaction mechanism. These elements have motivated us to divide the chemistry in the C-IFS-TS system into a tropospheric and stratospheric part. Note that there is only one set of transported atmospheric trace gases and only the position of the grid box above or below the tropopause determines if the tropospheric or stratospheric chemistry is applied.

The tropopause can be defined based on a different criteria. A common approach is to use dynamical criterion such as the isentropic potential vorticity (e.g., Thuburn and Craig, 1997) but this fails in regions of small absolute vorticity, notably in the tropics. A definition based on the lapse rate (WMO, 1957) is an alternative, but may not be well defined in the presence of multiple stable layers. We therefore choose to base our criterion on the chemical composition of the atmosphere considering that the tropopause is associated with sharp gradients in trace gases (e.g., Gaudel et al., 2015). This has the advantage that parcels with tropospheric/stratospheric composition can be traced dynamically, and the most appropriate chemistry scheme can be adopted to it. In our simulation we use a chemical definition of the tropopause level, where tropospheric grid cells are defined at O_3<200 ppb and CO>40 ppb, for P > 40 hPa.

For both troposphere (CB05) and stratosphere (BASCOE) the numerical solver is generated using the Kinetic Pre-Processor (KPP, Sandu and Sander, 2006) software. Specificaly we adopt the standard four-stages, third order Rosenbrock solver (Rodas3). This is different from the hard-coded Eulerian backward implicit solver as used in Flemming et al. (2015), and is motivated by the improved coding flexibility and accuracy.

Most of the gas phase reactions that take place both in the troposphere and stratosphere, such as NO_x and HO_x reactions, are simulated in identical ways in both chemistry schemes. It is worth mentioning that the tracers O^1D and O^3P, produced from O_3 and O_2 photolysis, are described implicitly in the troposphere, while they are treated explicitly in the stratosphere. For trace gases whose chemistry is currently neglected in the stratosphere (the NMHC's, PAN, Organic nitrate, SO_2) we adopt a 10-day decay rate to prevent spurious accumulation of these tracers in the stratosphere. Note that tropospheric halogen

Geosci. Model Dev. Discuss., doi:10.5194/gmd-2016-40, 2016
Manuscript under review for journal Geosci. Model Dev.
Published: 7 March 2016

chemistry, which contributes to ozone depletion in spring-time polar region and to changes in oxidative capacity in the tropical marine boundary layer (von Glasow and Crutzen, 2007) is currently neglected, even though related trace gases are available. By inspection of individual tracer fields we have ensured that the merging strategy does not result in spurious jumps at the interface between troposphere and stratosphere. In case of running the system with stratospheric chemistry only (C-IFS-S), all chemistry and emissions are switched off at altitudes below 400 hPa and replaced by surface boundary conditions.

The three options to run this type of C-IFS experiments and the computational cost are given in Table 2. As compared to the C-IFS-T experiments, the costs of running an experiment including full stratospheric chemistry with the C-IFS-TS system have increased by ~50%. The additional burden for transport due to the increase in the number of tracers only marginally increases the computational time, because of the efficiency of the semi-Lagrangian advection for multiple tracers. A test experiment where tropospheric and stratospheric chemistry were merged into a single reaction mechanism, where all reactions are activated in the whole atmosphere, led to an increase in costs by ~50% compared to C-IFS-TS, indicating the benefit of having separate solver codes for tropospheric and stratospheric chemistry. Finally this also allows for an easy switch between system setups.

2.3.1 Merging photolysis rates

For parameterization of the photolysis rates the Modified Band Approach (MBA, Williams et al., 2012) and the lookup table approach (Errera and Fonteyn, 2001) as have been optimized in the past for applications in the troposphere and stratosphere are retained, see Table 3. While for tropospheric conditions scattering and absorption properties of clouds and aerosol strongly impact the magnitude of photolysis rates and hence the local chemical composition, this is of less relevance in the stratosphere. Wavelengths shorter than 202 nm, on the other hand, are largely blocked by stratospheric ozone and oxygen and do not contribute to radiation in the troposphere (Williams et al., 2012). At higher altitudes these short wavelengths contribute to the Chapman cycle and to the break down of CH_4, CFC's and N_2O either directly or through oxidation by O^1D. Also the presence of sunlight at solar zenith angles (SZA) larger than 90° at high altitudes needs to be accounted for in the stratosphere but not necessarily in the troposphere. Solar radiation reaches the stratosphere earlier than the Earth's surface, due to the Earth's curvature which, amongst others, triggers the polar spring stratospheric ozone depletion.

Table 4 lists the photolysis rates that are active both in the troposphere and stratosphere. Photolysis rates for reactions occurring both in the troposphere and stratosphere are merged at the interface, in order to ensure a smooth transition between the two schemes. This is done by an interpolation at four model levels around the interface level between both parameterizations, for SZA<85°. For larger SZA the original value for the photolysis rate is retained in case of stratospheric chemistry, while it is switched off for the troposphere.

Note that even though the reaction rates have been merged, the products from the same photolytic reactions are sometimes different as a consequence of the different reaction mechanisms between the troposphere and stratosphere.

Geosci. Model Dev. Discuss., doi:10.5194/gmd-2016-40, 2016
Manuscript under review for journal Geosci. Model Dev.
Published: 7 March 2016

An example of the merging strategy is given in Fig. 1. It shows that at the interface for J O_3 and J NO_2 on average a small increase of the merged photolysis rate is seen towards lower altitudes, with the switch to MBA in the troposphere, which is a consequence of the combination of differences in the parameterizations. Even though such jumps are undesirable, no visible impact on local chemical composition was found.

2.3.2 Merging tracer transport

Tracer transport is treated identically for all individual chemical tracers. Since the semi-Lagrangian advection does not formally conserve mass (Flemming and Huijnen, 2011) a global mass fixer is applied (Diamantakis and Flemming, 2014) to all but a few tracers, including NO, NO_2 and H_2O. Rather than conserving mass during the advection step of the individual components NO and NO_2, this is enforced to a stratospheric NO_x tracer defined as the sum of NO and NO_2. While a chemical H_2O tracer is defined in the full atmosphere, in the troposphere H_2O mass mixing ratios are constrained by the humidity (q) simulated in the meteorological model in the IFS. Stratospheric H_2O (i.e. above the tropopause level) is governed by chemical production and loss. Stratospheric H_2O mass is not strictly conserved considering that the global advection errors essentially originate from the tropospheric part (where by far most H_2O mass is located with large spatial gradients), and should not affect the stratospheric H_2O mass budget (where total mass is much lower and H_2O mixing ratio gradients are much smoother).

3. Model setup and observations used

We have executed a run of C-IFS-TS for the period April 2008 until December 2009. Stratospheric ozone in C-IFS-TS is further compared to that of the C-IFS-T system (Flemming et al., 2015) which uses the ECMWF standard linear ozone scheme (version 2a, Cariolle and Teyssèdre, 2007) in the stratosphere.

We have initialized C-IFS-TS and CIFS-T runs on 1 April 2008 using assimilated concentration fields from the BASCOE system in the stratosphere for this date. The horizontal resolution of these runs is T255 (i.e. approx. 0.7° lon / lat) with 60 levels in the vertical. Meteorology is relaxed towards ERA-Interim.

The performance of C-IFS-TS has further been compared against the BASCOE-CTM (without data assimilation), using the same chemical mechanism and parameterizations as implemented in the C-IFS. The BASCOE-CTM is run with a resolution of 1.0° lon / lat similar to the resolution of C-IFS used here, and on the same vertical grid of 60 levels. It uses temperature, pressure and wind fields simulated by the C-IFS runs. Using the same dynamical fields together with an identical implementation of the chemistry code should allow to identify differences in the transport schemes between C-IFS and the BASCOE-CTM. Common chemical biases between both systems also point at issues in the chemical parameterization.

Geosci. Model Dev. Discuss., doi:10.5194/gmd-2016-40, 2016
Manuscript under review for journal Geosci. Model Dev.
Published: 7 March 2016

3.1 Observational data used for validation

We evaluate C-IFS-TS in terms of stratospheric O_3, NO_2, N_2O, CH_4, H_2O and HCl, and for this purpose use a range of observation-based products.

Total column O_3 is validated against KNMI's multi sensor reanalysis version 2 (MSR, van der A et al., 2015) which, for the 2008-2009 time period is based on Solar Backscattering Ultraviolet radiometer (SBUV/2), Global Ozone Monitoring Experiment (GOME), SCanning Imaging Absorption spectroMeter for Atmospheric CartograpHY (SCIAMACHY) and Ozone Monitoring Instrument (OMI) observations. The satellite retrieval products used in the MSR are bias-corrected with respect to Brewer and Dobson Spectrophotometers to remove discrepancies between the different satellite data sets. The uncertainty in the product, as quantified by the bias of the observation-minus-analysis statistics, is in general less than 1 DU.

O_3 profiles are compared to ozonesonde data that are acquired from the World Ozone and Ultaviolet radiation Data Centre (WOUDC). The precision of the ozonesondes is on the order of 5% in the stratosphere (Hassler et al., 2015), when based on electrochemical concentration cell (ECC) devices (~85% of all soundings). Larger random errors (5-10%) are found for other sonde types, and in the presence of steep gradients and where the ozone amount is low. Sondes at 19, 12, 2 and 1 individual stations are used for the evaluation over northern hemisphere midlatitudes, tropics, southern hemisphere midlatitudes and Antarctic, respectively.

Stratospheric NO_2 columns are compared to observational data from the SCIAMACHY (Bovensmann et al., 1999) UV–VIS (ultraviolet–visible) and NIR (near-infrared) sensor onboard the Envisat satellite. The satellite retrievals are based on applying the Differential Optical Absorption Spectroscopy (DOAS) (Platt and Stutz, 2008) method to a 425-450 nm wavelength window. Stratospheric NO_2 columns from SCIAMACHY are in fact total columns derived using a stratospheric air mass factor (Richter et al., 2005). To minimize the impact of the troposphere, only data over the clean Pacific region are used (180°E - 220°E). Still, the amount considered here as being stratospheric includes a weighted part of the tropospheric background NO_2. Monthly mean stratospheric NO_2 columns are associated with relative uncertainties of roughly 5-10% and an additional absolute uncertainty of 1×10^{14} molec cm^{-2}. To account for differences in observation and model output time, simulations are interpolated linearly to the equator crossing time of SCIAMACHY (10:00 LT). In addition, only model data for which satellite observations exist are included in the corresponding comparisons.

Furthermore, satellite-based observations are used from the Atmospheric Chemistry Experiment - Fourier Transform Spectrometer (ACE-FTS), onboard of the Canadian satellite mission SCISAT-1 (first Science Satellite, Bernath et al., 2005). This is a high spectral resolution Fourier transform spectrometer operating with a Michelson interferometer. Vertical profiles of atmospheric volume mixing ratios of trace constituents are retrieved from the occultation spectra, as described in Boone et al. (2005), with a vertical resolution of 3–4 km at maximum. Here we use level 2 retrievals (version 3.0) of N_2O and CH_4.

ACE-FTS N_2O observations between 6 and 30 km are within ±15% compared against independent observations, while above they agree to within ±4 ppbv (Strong et al., 2008). The uncertainty in ACE-FTS CH_4 observations is within 10% in the upper

Geosci. Model Dev. Discuss., doi:10.5194/gmd-2016-40, 2016
Manuscript under review for journal Geosci. Model Dev.
Published: 7 March 2016

troposphere – lower stratosphere, and within 25% in the middle and higher stratosphere up to the lower mesosphere (<60 km) (De Mazière et al. 2008).

Model results are also compared with observations of O_3 (Ceccherini et al., 2008), HNO_3 (Wang et al., 2007) and NO_2 (Wetzel et al., 2007) retrieved from limb emission spectra recorded by the Michelson Interferometer for Passive Atmospheric Sounding (MIPAS) onboard the European satellite Envisat, and with observations of H_2O (Read et al., 2007) and HCl (Froidevaux et al., 2008) retrieved from the Microwave Limb Sounder (MLS) onboard the satellite Aura.

MIPAS random and systematic errors for various trace gases are reported by Raspollini et al. (2013). For NO_2 between 25 and 50 km altitude these are below 10 and 20% respectively. For HNO_3 between 15 and 30 km, these are below 8 and 15% while for O_3 between 20 and 55 these are below 5 and 10%. At 15 km, these errors increase to 10 and 20%, respectively. The MLS error budget is reported in Livesey et al. (2011). For HCl observations between 1-20 hPa the precision and accuracy are below 10 and 15% respectively. Between 46 and 100 hPa, these are below 0.3 and 0.2 ppbv, respectively. For H_2O between 0.46 and 100 hPa, precision and accuracy are below 15 and 8%.

4. Model evaluation

Fig. 2 shows the zonal mean O_3 total columns against the MSR at various latitude bands. It shows that for the extra-tropical mid-latitudes the positive and negative biases remain below 20 DU (6%), while for the tropics the bias increases towards -18 DU (8%) at the end of the model simulation. Over Antarctica (70S – 90S) the zonal, monthly mean average bias is generally less than 20 DU, except for the ozone hole period when the minimum ozone is underestimated by up to 35 DU (25%). In contrast, the Cariolle scheme shows an over-estimation of O_3 column outside the ozone hole period, and a relatively appropriate magnitude of the ozone minimum. While over the northern hemisphere C-IFS-TS shows a clear improvement compared to C-IFS-T with Cariolle, for the tropical and southern hemisphere both versions show a similar performance.

Closer inspection of O_3 profiles against sondes averaged over the NH-mid latitudes, tropics and SH-mid latitudes for the DJF and JJA seasons (Figures 3 and 4) also shows reduced biases most prominently visible at the 10-30 hPa altitude range in the sub-tropics for C-IFS-TS. Nevertheless, this experiment still shows a positive bias near the ozone maximum in terms of partial pressure (~50 hPa) and also at lower altitudes during the northern hemispheric spring season. In the tropics the use of the full stratospheric chemistry implies a slight degradation against the linear scheme around the ozone maximum, where the Cariolle parameterization is very well tuned while the negative bias in the lower stratosphere, as also found in C-IFS-T, is not improved.

For the 2009 Antarctic ozone hole season (Fig. 5) the C-IFS-TS shows a positive bias at ~100 hPa for August and September, but the depth of the ozone hole is well modelled in October. During the closure phase in November and December the O_3 variability with altitude is better captured in C-IFS-TS than in C-IFS-T. The evaluation of the zonal mean ozone concentrations against MIPAS observations shows good general agreement, Fig. 6, with small biases of similar magnitude as the ones for the BASCOE-CTM simulation.

Geosci. Model Dev. Discuss., doi:10.5194/gmd-2016-40, 2016
Manuscript under review for journal Geosci. Model Dev.
Published: 7 March 2016

The assessment of NO_2 against MIPAS daytime NO_2 observations, acquired by sampling the ascending orbits from Envisat, shows good agreement with both models. Also the C-IFS-TS describes well the seasonal variation in zonal mean stratospheric NO_2 columns at different latitude bands, Fig. 7, with monthly mean biases with respect to the SCIAMACHY observations of less than $\pm 0.5 \times 10^{15}$ molec cm^{-2} in the tropics and at mid-latitudes.

However, a positive NO_2 bias with respect to night-time MIPAS NO_2 observations appears larger for C-IFS-TS than for the BASCOE-CTM (Fig. 6). In contrast, this figure also shows a negative bias in HNO_3 with respect to MIPAS observations in both the BASCOE-CTM and C-IFS-TS, again more marked in the C-IFS experiment. Considering that daytime NO_2 bias in C-IFS-TS is small and similar to that for BASCOE-CTM, the larger negative bias in C-IFS HNO_3 is likely not caused by biases in its chemical precursors.

Fig. 8 shows an evaluation of N_2O and CH_4 profiles during September 2009 against observations by ACE-FTS. Owing to their long lifetimes these trace gases are good markers for the model ability to describe (vertical) transport. Moreover, N_2O is the main source of reactive nitrogen in the stratosphere while CH_4 is one of the main precursors for stratospheric water vapour. The figure suggests reasonable profile shapes for both CH_4 and N_2O in the upper stratosphere (10 hPa and higher), which is also rather similar as found in the BASCOE-CTM control run. Even though the absolute difference between C-IFS N_2O and observations from MIPAS and MLS is somewhat different in absolute terms than found for the evaluation against ACE-FTS, the general features are very similar.

At lower altitudes (100-10 hPa) C-IFS-TS N_2O and CH_4 shows larger discrepancies to the observations, and to the BASCOE-CTM run with an over-estimation most prominently around 30 hPa in the tropics and SH-mid latitudes, suggesting too much vertical transport within the middle and lower stratosphere. This feature could also contribute to the positive biases seen in O_3 at ~20 hPa in Figures 3 and 4.

Fig. 9 shows a good consistency between H_2O modelled by C-IFS-TS and the BASCOE-CTM results, albeit with a slight negative bias with respect to MLS observations above 5 hPa, and a positive bias around 30 hPa in the tropics, associated with corresponding biases in CH_4. This figure also shows globally a good agreement between HCl modelled by C-IFS-TS and MLS observations, although with a positive bias of 0.8 ppbv confined in the region of ozone depletion above Antarctica.

5. Conclusions

We have presented a model description and benchmark evaluation of an extension of the C-IFS system with stratospheric ozone chemistry of the BASCOE model added to the already existing tropospheric scheme CB05, referred to as C-IFS-CB05-BASCOE, or C-IFS-TS in short. In our approach we have retained a separate treatment for tropospheric and stratospheric chemistry, and select the most appropriate scheme depending on the altitude with respect to the tropopause level. This has the advantage that parameterizations which are optimized for tropospheric and stratospheric chemistry, respectively, can be retained, which also substantially reduces the computational costs of the chemical solver compared to an approach where all reactions are activated in the whole atmosphere. Also, it allows for an easy switch between system

Geosci. Model Dev. Discuss., doi:10.5194/gmd-2016-40, 2016
Manuscript under review for journal Geosci. Model Dev.
Published: 7 March 2016

setups. To avoid jumps in tracer concentrations at the interface the consistency in gas-phase reaction rates has been verified while the photolysis rates from the two parameterizations are interpolated across the interface.

An evaluation of a 1.5 year simulation of C-IFS-TS indicates good performance of the system in terms of stratospheric ozone, of similar quality as BASCOE-CTM model results. The O_3 total columns show biases mostly smaller than ±20 DU when compared to the MSR-v2. Also the profiles were generally well captured, and show an improvement with respect to the C-IFS-T linear ozone scheme in the stratosphere over mid-latitudes. The depth and variability of the ozone hole over Antarctica is modelled well.

Also evaluation of other trace gases (NO_2, HNO_3, CH_4, N_2O, HCl) against observations derived from various satellite retrievals (SCIAMACHY, ACE-FTS, MIPAS, MLS) indicates a good performance. But for CH_4 and N_2O a larger error with respect to limb-sounding retrievals was found at around 30 hPa than the BASCOE-CTM. This could point at too fast vertical transport within the middle and lower stratosphere in the C-IFS framework.

This benchmark model evaluation of C-IFS-TS marks a first step towards merging tropospheric and stratospheric chemistry within IFS, aiming at daily operational forecasts of composition for the entire atmosphere. Future work will focus on the following aspects:

- Chemical data-assimilation: initial tests with data-assimilation of O_3 total column and profile retrievals suggest that stratospheric ozone is successfully constrained in C-IFS-TS. However, observational constraints on other components driving ozone chemistry are currently lacking in the assimilation system. Our extension opens the possibility for assimilation of additional tracers such as N_2O and HCl. However, for the 4D-VAR assimilation of short-lived species such as NO_2 and ClO an adjoint chemistry module would be required as implemented the BASCOE DA system.
- Alignment of the reaction mechanism and photolysis rates: while at current stage the gas-phase and photolytic reaction rates of the parent schemes are retained, we foresee a further integration to ensure better alignment of the chemical mechanisms. Especially the existing jumps in photolysis rates as a consequence of the different parameterizations are not desirable, even though they are not harmful for model stability nor visibly lead to any degradation in model performance. The alignment in terms of gas-phase reaction rate expressions can be achieved by the introduction of the KPP solver in C-IFS, for both tropospheric and stratospheric chemistry, which allows for a better traceable model development than the hard-coded Euler Backward Integration solver as adopted in Flemming et al. (2015).
- Extension of tropospheric and stratospheric chemistry schemes: the availability of a comprehensive set of tracer fields allows for a relatively easy extension of the tropospheric reaction mechanism by including selective reactions originating from the stratospheric chemistry, and vice versa. Examples are the introduction of halogen chemistry in the troposphere (von Glasow and Crutzen, 2007), or SO2 conversion to sulphate aerosol in the stratosphere, relevant in case of strong volcanic events (Bândă, et al., 2015).
- Optimization of solver efficiency: even though the use of KPP has simplified the code maintenance and may result in a higher numerical accuracy of the solution, it also caused a considerable slow-down of the numerical efficiency as compared to the Euler Backward Integration solver, as that solver had been optimized for tropospheric ozone chemistry in C-IFS-

Geosci. Model Dev. Discuss., doi:10.5194/gmd-2016-40, 2016
Manuscript under review for journal Geosci. Model Dev.
Published: 7 March 2016

CB05. Solutions could be an optimization of the initial chemical time step for the KPP solver, depending on prevailing chemical and physical conditions, and an optimization of the automated solver code, which allows for a more efficient code structure (KP4, Jöckel et al., 2010).

In summary, the extension towards stratospheric chemistry in C-IFS broadens its ability for forecast and assimilation of stratospheric composition, which is beneficial to the monitoring capabilities in CAMS, and may also contribute to advances in meteorological forecasting of the ECMWF IFS model in the future.

Code availability

The C-IFS source code is integrated into ECWMF's IFS code, which is available subject to a licence agreement with ECMWF, see also Flemming et al. (2015) for details. The stratospheric chemistry module of C-IFS was originally developed in the framework of BASCOE. Readers interested in the BASCOE code can contact the developers through http://bascoe.oma.be.

Geosci. Model Dev. Discuss., doi:10.5194/gmd-2016-40, 2016
Manuscript under review for journal Geosci. Model Dev.
Published: 7 March 2016

Geoscientific Model Development Discussions

Appendix A

Table A1. Trace gases in C-IFS-TS, along with their chemically active domain: troposphere (Trop), stratosphere (Strat) or both (Glb).

Short name	Long name	Active domain
O3	ozone	Glb
H2O2	Hydrogen peroxide	Glb
HO2	Hydroperoxy radical	Glb
OH	Hydroxyl radical	Glb
CH4	methane	Glb
CO	Carbon monoxide	Glb
CH2O	formaldehyde	Glb
CH3O2	Methylperoxy radical	Glb
CH3OOH	methylperoxide	Glb
NO	Nitrogen monoxide	Glb
NO2	Nitrogen dioxide	Glb
NO3	Nitrate radical	Glb
HNO3	Nitric acid	Glb
HO2NO2	Pernitric acid	Glb
N2O5	Dinitrogen pentoxide	Glb
PAR	paraffins	Trop

Geosci. Model Dev. Discuss., doi:10.5194/gmd-2016-40, 2016
Manuscript under review for journal Geosci. Model Dev.
Published: 7 March 2016

C2H4	ethene	Trop
OLE	olefins	Trop
ALD2	aldehydes	Trop
PAN	Peroxyacetyl nitrate	Trop
ROOH	peroxides	Trop
ONIT	Organic nitrates	Trop
SO2	Sulfur dioxide	Trop
SO4	sulfate	Trop
DMS	Dimethyl sulfide	Trop
NO3_A	nitrate	Trop
NH3	ammonia	Trop
NH4	ammonium	Trop
MSA	Methanesulfonic acid	Trop
CH3COCHO	methylglyoxal	Trop
C2O3	Peroxyacetyl radical	Trop
ROR	Organic ethers	Trop
RXPAR	PAR budget corrector	Trop
XO2	NO to NO2 operator	Trop
XO2N	NO to alkyl nitrate operator	Trop
CH3OH	methanol	Trop

Geosci. Model Dev. Discuss., doi:10.5194/gmd-2016-40, 2016
Manuscript under review for journal Geosci. Model Dev.
Published: 7 March 2016

HCOOH	Formic acid	Trop
MCOOH	Methacrylic acid	Trop
C2H6	ethane	Trop
C2H5OH	ethanol	Trop
C3H8	propane	Trop
C3H6	propene	Trop
C5H8	isoprene	Trop
C10H16	terpenes	Trop
CH3COCH3	acetone	Trop
ISPD	Methacrolein MVK	Trop
ACO2	Acetone product	Trop
IC3H7O2	IC3H7O2	Trop
HYPROPO2	HYPROPO2	Trop
NH2	amine	Trop
Rn	radon	Glb
Pb	lead	Trop
CH3	Methyl radical	Strat
CH3O	Methoxy radical	Strat
HCO	Formyl radical	Strat
N2O	Nitrous oxide	Strat

Geosci. Model Dev. Discuss., doi:10.5194/gmd-2016-40, 2016
Manuscript under review for journal Geosci. Model Dev.
Published: 7 March 2016

H2O	water	Strat
OCLO	Chlorine dioxide	Strat
HCL	Hydrogen chloride	Strat
CLONO2	chlorine_nitrate	Strat
HOCL	Hypochlorous acid	Strat
CL2	chlorine	Strat
HBR	Hydrogen bromide	Strat
BRONO2	Bromine nitrate	Strat
CL2O2	dichlorine_dioxide	Strat
HOBR	Hypobromous acid	Strat
BRCL	Bromine monochloride	Strat
CFC11	trichlorofluoromethane	Strat
CFC12	dichlorodifluoromethane	Strat
CFC113	trichlorotrifluoroethane	Strat
CFC114	1,2-Dichlorotetrafluoroethane	Strat
CFC115	Chloropentafluoroethane	Strat
CCL4	tetrachloromethane	Strat
CLNO2	Chloro(oxo)azane oxide	Strat
CH3CCL3	Methyl chloroform	Strat
CH3CL	Methyl chloride	Strat

Geosci. Model Dev. Discuss., doi:10.5194/gmd-2016-40, 2016
Manuscript under review for journal Geosci. Model Dev.
Published: 7 March 2016

HCFC22	chlorodifluoromethane	Strat
CH3BR	Methyl bromide	Strat
HF	Hydrofluoric acid	Strat
HA1301	Bromotrifluoromethane	Strat
HA1211	Bromochlorodifluoromethane	Strat
CHBR3	Bromoform	Strat
CLOO	Asymmetric chlorine dioxide radical	Strat
O	Oxygen atom	Strat
O1D	Excited oxygen atom	Strat
N	Nitrogen atom	Strat
CLO	Chlorine monoxide	Strat
CL	Chlorine atom	Strat
BR	Bromine atom	Strat
BRO	Bromine monoxide	Strat
H	Hydrogen atom	Strat
H2	hydrogen	Strat
CO2	carbondioxide	Strat
BR2	Bromine atomic ground state	Strat
CH2BR2	dibromomethane	Strat

Geosci. Model Dev. Discuss., doi:10.5194/gmd-2016-40, 2016
Manuscript under review for journal Geosci. Model Dev.
Published: 7 March 2016

Geoscientific Model Development Discussions

Acknowledgments

MACC III was funded by the European Union's Seventh Framework Programme (FP7) under Grant Agreement no. 283576. We are grateful to the World Ozone and Ultraviolet Radiation Data Centre (WOUDC) for providing ozone sonde observations and to the GOME-2, MIPAS, ACE-FTS and MLS teams for providing satellite observations.

References

Atkinson, R., Baulch, D. L., Cox, R. A., Crowley, J, N., Hampson, R. F., Hynes, R. G., Jenkin, M. E., Rossi, M. J. and Troe, J.: evaluated kinetic and photochemical data for atmospheric chemistry: Volume I – gas phase reactions of Ox, HOx, NOx and SOx, species, Atmos. Chem. Phys., 4, 1461–1738, doi:10.5194/acp-4-1461-2004, 2004.

Atkinson, R., Baulch, D. L., Cox, R. A., Crowley, J. N., Hampson, R. F., Hynes, R. G., Jenkin, M. E., Rossi, M. J., Troe, J., and IUPAC Subcommittee: Evaluated kinetic and photochemical data for atmospheric chemistry: Volume II – gas phase reactions of organic species, Atmos. Chem. Phys., 6, 3625–4055, doi:10.5194/acp-6-3625-2006, 2006.

Baldwin, M. P., Gray, L. J., Dunkerton, T. J., Hamilton, K., Haynes, P. H., Randel, W. J., Holton, J. R., Alexander, M. J., Hirota, I., Horinouchi, T., Jones, D. B. A., Kinnersley, J. S., Marquardt, C., Sato, K. and Takahashi, M.: The quasi-biennial oscillation, Rev. Geophys., 39(2), 179–229, doi:10.1029/1999RG000073, 2001.

Bândă, N., Krol, M., van Weele, M., van Noije, T., Le Sager, P., and Röckmann, T.: Can we explain the observed methane variability after the Mount Pinatubo eruption?, Atmos. Chem. Phys. Discuss., 15, 19111-19160, doi:10.5194/acpd-15-19111-2015, 2015.

Benedetti, A., Morcrette, J.-J., Boucher, O., Dethof, A., Engelen, R. J., Fisher, M., Flentje, H., Huneeus, N., Jones, L.,Kaiser, J. W., Kinne, S., Mangold, A., Razinger, M.,Simmons, A. J., Suttie, M., and the GEMS-AER team: Aerosol analysis and forecast in the European Centre for Medium-Range Weather Forecasts Integrated Forecast System: 2. Data assimilation, J. Geophys. Res., 114, D13205, doi:10.1029/2008JD011115, 2009.

Bovensmann, H., Burrows, J. P., Buchwitz, M., Frerick, J., Noël, S., Rozanov, V. V., Chance, K. V., and Goede, A. P. H.: SCIAMACHY: Mission Objectives and Measurement Modes, J. Atmos. Sci., 56, 127–150, 1999.

Brasseur, G., A. Smith, R. Khosravi, T. Huang, S. Walters, S. Chabrillat and Kockarts, G.: Natural and human-induced perturbations in the middle atmosphere: A short tutorial, In Atmospheric Science Across the Stratopause, pages 7-20, AGU Geophys. Monograph, vol. 123, 2000.

Cariolle, D. and Morcrette, J.-J.: A linearized approach to the radiative budget of the stratosphere: Influence of the ozone distribution, Geophys. Res. Lett., 33, L05806, doi:10.1029/2005GL025597, 2006.

Cariolle, D. and Teyssèdre, H.: A revised linear ozone photochemistry parameterization for use in transport and general circulation models: multi-annual simulations, Atmos. Chem. Phys., 7, 2183-2196, doi:10.5194/acp-7-2183-2007, 2007.

Ceccherini, S., Cortesi, U., Verronen, P. T., and Kyrölä, E.: Technical Note: Continuity of MIPAS-ENVISAT operational ozone data quality from full- to reduced-spectral-resolution operation mode, Atmospheric Chemistry and Physics, 8, 2201–2212, doi:10.5194/acp-8-2201-2008, 2008.

Chabrillat, S. and Fonteyn, D.: Modelling long-term changes of mesospheric temperature and chemistry, Adv. Space Res., 32, 9, pages 1689-1700, 2003.

Chipperfield, M. P., Dhomse, S. S., Feng, W., McKenzie, R. L., Velders, G.J.M., Pyle, J. A.: Quantifying the ozone and ultraviolet benefits already achieved by the Montreal Protocol. Nat Commun., 6, http://dx.doi.org/10.1038/ncomms8233, 2015.

de Grandpré J., Ménard R., Rochon Y., Charette C., Chabrillat S. and Robichaud A. : Radiative impact of ozone on temperature predictability in a coupled chemistry-dynamics data assimilation system, Monthly Weather Rev., 137, 679-692, doi:10.1175/2008MWR2572.1, 2009.

De Mazière, M., Vigouroux, C., Bernath, P. F., Baron, P., Blumenstock, T., Boone, C., Brogniez, C., Catoire, V., Coffey, M., Duchatelet, P., Griffith, D., Hannigan, J., Kasai, Y., Kramer, I., Jones, N., Mahieu, E., Manney, G. L., Piccolo, C., Randall, C., Robert, C., Senten, C., Strong, K., Taylor, J., Tétard, C., Walker, K. A., and Wood, S.: Validation of ACE-FTS v2.2 methane profiles from the upper troposphere to the lower mesosphere, Atmos. Chem. Phys., 8, 2421–2435, doi:10.5194/acp-8-2421-2008, http://www.atmos-chem-phys.net/8/2421/ 2008/, 2008.

Engelen, R. J., Serrar, S., and Chevallier, F.: Four-dimensional data assimilation of atmospheric CO2 using AIRS observations, J. Geophys. Res., 114, D03303, doi:10.1029/2008JD010739, 2009.

Errera, Q. and Fonteyn, D.: Four-dimensional variational chemical assimilation of CRISTA stratospheric measurements, J. Geophys. Res., 106, 12,253-12, 265, 2001.

Errera, Q., Daerden, F., Chabrillat, S., Lambert, J. C., Lahoz, W. A., Viscardy, S., Bonjean, S., and Fonteyn, D.: 4D-Var assimilation of MIPAS chemical observations: ozone and nitrogen dioxide analyses, Atmos. Chem. Phys., 8, 6169-6187, doi:10.5194/acp-8-6169-2008, 2008.

Eskes, H., Huijnen, V., Arola, A., Benedictow, A., Blechschmidt, A.-M., Botek, E., Boucher, O., Bouarar, I., Chabrillat, S., Cuevas, E., Engelen, R., Flentje, H., Gaudel, A., Griesfeller, J., Jones, L., Kapsomenakis, J., Katragkou, E., Kinne, S., Langerock, B., Razinger, M., Richter, A., Schultz, M., Schulz, M., Sudarchikova, N., Thouret, V., Vrekoussis, M., Wagner, A., and Zerefos, C.: Validation of reactive gases and aerosols in the MACC global analysis and forecast system, Geosci. Model Dev., 8, 3523-3543, doi:10.5194/gmd-8-3523-2015, 2015a.

Flemming, J., Inness, A., Flentje, H., Huijnen, V., Moinat, P., Schultz, M. G., and Stein, O.: Coupling global chemistry transport models to ECMWF's integrated forecast system, Geosci. Model Dev., 2, 253-265, doi:10.5194/gmd-2-253-2009, 2009.

Flemming, J., Inness, A., Jones, L., Eskes, H. J., Huijnen, V., Schultz, M. G., Stein, O., Cariolle, D., Kinnison, D., and Brasseur, G.: Forecasts and assimilation experiments of the Antarctic ozone hole 2008, Atmos. Chem. Phys., 11, 1961–1977, doi:10.5194/acp-11-1961-2011, 2011 .

Flemming, J., Huijnen, V., Arteta, J., Bechtold, P., Beljaars, A., Blechschmidt, A.-M., Diamantakis, M., Engelen, R. J., Gaudel, A., Inness, A., Jones, L., Josse, B., Katragkou, E., Marecal, V., Peuch, V.-H., Richter, A., Schultz, M. G., Stein, O., and Tsikerdekis, A.: Tropospheric chemistry in the Integrated Forecasting System of ECMWF, Geosci. Model Dev., 8, 975-1003, doi:10.5194/gmd-8-975-2015, 2015.

Flemming, J. and Huijnen, V.: IFS Tracer Transport Study, MACC Deliverable G-RG 4.2, Tech. rep., ECMWF, available at: http://www.gmes-atmosphere.eu/documents/deliverables/g-rg/ifs_transport_study.pdf (last access: 15 December 2015), 2011.

Fonteyn, D. and Larsen, N.: Detailed PSC formation in a two-dimensional chemical transport model of thestratosphere, Ann. Geophys., 14, 315–328, 1996.

Froidevaux, L., Jiang, Y., Lambert, A., Livesey, N., Read, W., Waters, J., Fuller, R., Marcy, T., Popp, P., Gao, R., et al.: Validation of Aura microwave limb sounder HCl measurements, Journal of Geophysical Research: Atmospheres (1984–2012), 113, 2008.

Gaudel, A., Clark, H., Thouret, V., Jones, L., Inness, A., Flemming, J., Stein, O., Huijnen, V., Eskes, H., Nédélec, P., Boulanger, D.: On the use of MOZAIC-IAGOS data to assess the ability of the MACC reanalysis to reproduce the distribution of ozone and CO in the UTLS over Europe. Tellus B, 67, 27955. doi:http://dx.doi.org/10.3402/tellusb.v67.27955, 2015.

Geer, A. J., Lahoz, W. A., Bekki, S., Bormann, N., Errera, Q., Eskes, H. J., Fonteyn, D., Jackson, D. R., Juckes, M. N., Massart, S., Peuch, V.-H., Rharmili, S., and Segers, A.: The ASSET intercomparison of ozone analyses: method and first results, Atmos. Chem. Phys., 6, 5445-5474, 2006.

Hanson, D. R. and Ravishankara, A. R.: Reactive Uptake of ClONO2 onto Sulfuric Acid Due to Reaction with HCl and H2O, J. Phys. Chem., 98, 5728–5735, doi:10.1021/j100073a026, 1994.

Hassler, B., Petropavlovskikh, I., Staehelin, J., August, T., Bhartia, P. K., Clerbaux, C., Degenstein, D., Mazière, M. De, Dinelli, B. M., Dudhia, A., Dufour, G., Frith, S. M., Froidevaux, L., Godin-Beekmann, S., Granville, J., Harris, N. R. P., Hoppel, K., Hubert, D., Kasai, Y., Kurylo, M. J., Kyrölä, E., Lambert, J.-C., Levelt, P. F., McElroy, C. T., McPeters, R. D., Munro, R., Nakajima, H., Parrish, A., Raspollini, P., Remsberg, E. E., Rosenlof, K. H., Rozanov, A., Sano, T., Sasano, Y., Shiotani, M., Smit, H. G. J., Stiller, G., Tamminen, J., Tarasick, D. W., Urban, J., van der A, R. J., Veefkind, J. P., Vigouroux, C., von Clarmann, T., von Savigny, C., Walker, K. A., Weber, M., Wild, J., and Zawodny, J. M.: Past changes in the vertical distribution of ozone – Part 1: Measurement techniques, uncertainties and availability, Atmos. Meas. Tech., 7, 1395-1427, doi:10.5194/amt-7-1395-2014, 2014.

Im, U., R. Bianconi, E. Solazzo, I. Kioutsioukis, A. Badia, A. Balzarini, R. Baro, R. Bellasio, D. Brunner, C. Chemel, G. Curci, J. Flemming, R. Forkel, L. Giordano, P. Jimenez-Guerrero, M. Hirtl, A. Hodzic, L. Honzak, O. Jorba, C. Knote, J.J.P. Kuenen, P.A. Makar, A. Manders-Groot, L. Neal, J.L. Perez, G. Pirovano, G. Pouliot, R. San Jose, N. Savage, W. Schröder, R.S. Sokhi, D. Syrakov, A. Torian, P. Tuccella, K. Werhahn, R. Wolke, K. Yahya, R. Žabkar, Y. Zhang, J. Zhang, C. Hogrefe, S. Galmarini. Evaluation of operational online-coupled regional air quality models over Europe and

North America in the context of AQMEII phase2. Part I: ozone. Atmos. Environ., 115 (2015), pp. 404–420 http://dx.doi.org/10.1016/j.atmosenv.2014.09.042

Hollingsworth, A., Engelen, R.J., Textor, C., Benedetti, A., Boucher, O. , Chevallier, F., Dethof, A., Elbern, H., Eskes, H., Flemming, J., Granier, C., Kaiser, J.W. , Morcrette, J.-J., Rayner, P., Peuch, V.H., Rouil, L., Schultz, M.G.,. Simmons, A.J and The GEMS Consortium: Toward a Monitoring and Forecasting System For Atmospheric Composition: The GEMS Project. Bull. Amer. Meteor. Soc., 89, 1147-1164, 2008.

Huijnen, V., Williams, J., van Weele, M., van Noije, T., Krol, M., Dentener, F., Segers, A., Houweling, S., Peters, W., de Laat, J., Boersma, F., Bergamaschi, P., van Velthoven, P., Le Sager, P., Eskes, H., Alkemade, F., Scheele, R., Nédélec, P., and Pätz, H.-W.: The global chemistry transport model TM5: description and evaluation of the tropospheric chemistry version 3.0, Geosci. Model Dev., 3, 445-473, doi:10.5194/gmd-3-445-2010.

Huijnen, V., Williams, J. E., and Flemming, J.: Modeling global impacts of heterogeneous loss of HO2 on cloud droplets, ice particles and aerosols, Atmos. Chem. Phys. Discuss., 14, 8575-8632, doi:10.5194/acpd-14-8575-2014, 2014.

Inness, A., Blechschmidt, A.-M., Bouarar, I., Chabrillat, S., Crepulja, M., Engelen, R. J., Eskes, H., Flemming, J., Gaudel, A., Hendrick, F., Huijnen, V., Jones, L., Kapsomenakis, J., Katragkou, E., Keppens, A., Langerock, B., de Mazière, M., Melas, D., Parrington, M., Peuch, V. H., Razinger, M., Richter, A., Schultz, M. G., Suttie, M., Thouret, V., Vrekoussis, M., Wagner, A., and Zerefos, C.: Data assimilation of satellite-retrieved ozone, carbon monoxide and nitrogen dioxide with ECMWF's Composition-IFS, Atmos. Chem. Phys., 15, 5275-5303, doi:10.5194/acp-15-5275-2015, 2015.

Jöckel, P., Kerkweg, A., Pozzer, A., Sander, R., Tost, H., Riede, H., Baumgaertner, A., Gromov, S., and Kern, B.: Development cycle 2 of the Modular Earth Submodel System (MESSy2), Geosci. Model Dev., 3, 717-752, doi:10.5194/gmd-3-717-2010, 2010.

Kaiser, J. W., Heil, A., Andreae, M. O., Benedetti, A., Chubarova, N., Jones, L., Morcrette, J.-J., Razinger, M., Schultz, M. G., Suttie, M., and van der Werf, G. R.: Biomass burning emissions estimated with a global fire assimilation system based on observed fire radiative power, Biogeosciences, 9, 527-554, doi:10.5194/bg-9-527-2012, 2012.

Lahoz, W. A., Errera, Q., Viscardy, S., and Manney G. L.: The 2009 stratospheric major warming described from synergistic use of BASCOE water vapour analyses and MLS observations, Atmos. Chem. Phys. 11, 4689-4703, 2011.

Lefever, K., van der A, R., Baier, F., Christophe, Y., Errera, Q., Eskes, H., Flemming, J., Inness, A., Jones, L., Lambert, J.-C., Langerock, B., Schultz, M. G., Stein, O., Wagner, A., and Chabrillat, S.: Copernicus stratospheric ozone service, 2009–2012: validation, system intercomparison and roles of input data sets, Atmos. Chem. Phys., 15, 2269-2293, doi:10.5194/acp-15-2269-2015, 2015.

Livesey, N. J., Read, W. G., Froidevaux, L., Lambert, A., Manney, G. L., Pumphrey, H. C., Santee, M. L., Schwartz, M. J., Wang, S., Cofield, R. E., Cuddy, D. T., Fuller, R. A., Jarnot, R. F., Jiang, J. H., Knosp, B. W., Stek, P. C., Wagner, P. A., and Wu, D. L.: Earth Observing System (EOS) Aura Microwave Limb Sounder (MLS) Version 3.3 Level 2 data quality and description document, Tech. Rep. D-33509, JPL, 2011.

Madronich, S. and Flocke, S.: The Role of Solar Radiation in Atmospheric Chemistry, in: Environmental Photochemistry, edited by Boule, P., vol. 2 / 2L of The Handbook of Environmental Chemistry, pp. 1–26, Springer Berlin Heidelberg, doi:10.1007/978-3-540-69044-3_1, 1999.

Manney, G. L., Lawrence, Z. D., Santee, M. L., Livesey, N. J., Lambert, A., and Pitts, M. C.: Polar processing in a split vortex: Arctic ozone loss in early winter 2012/2013, Atmos. Chem. Phys., 15, 5381-5403, doi:10.5194/acp-15-5381-2015, 2015.

Marécal, V., Peuch, V.-H., Andersson, C., Andersson, S., Arteta, J., Beekmann, M., Benedictow, A., Bergström, R., Bessagnet, B., Cansado, A., Chéroux, F., Colette, A., Coman, A., Curier, R. L., Denier van der Gon, H. A. C., Drouin, A., Elbern, H., Emili, E., Engelen, R. J., Eskes, H. J., Foret, G., Friese, E., Gauss, M., Giannaros, C., Guth, J., Joly, M., Jaumouillé, E., Josse, B., Kadygrov, N., Kaiser, J. W., Krajsek, K., Kuenen, J., Kumar, U., Liora, N., Lopez, E., Malherbe, L., Martinez, I., Melas, D., Meleux, F., Menut, L., Moinat, P., Morales, T., Parmentier, J., Piacentini, A., Plu, M., Poupkou, A., Queguiner, S., Robertson, L., Rouïl, L., Schaap, M., Segers, A., Sofiev, M., Thomas, M., Timmermans, R., Valdebenito, Á., van Velthoven, P., van Versendaal, R., Vira, J., and Ung, A.: A regional air quality forecasting system over Europe: the MACC-II daily ensemble production, Geosci. Model Dev. Discuss., 8, 2739-2806, doi:10.5194/gmdd-8-2739-2015, 2015.

Maycock, A. C., Keeley, S. P. E., Charlton-Perez, A. J., and Doblas-Reyes, F. J.: Stratospheric circulation in seasonal forecasting models: implications for seasonal prediction, Clim. Dynam., 36, 309–321, doi:10.1007/s00382-009-0665-x, 2011.

McGregor, J. L.: C-CAM Geometric Aspects and Dynamical Formulation, Tech. Rep. 70, CSIRO Atmospheric Research, Aspendale, Victoria, 2005.

Monge-Sanz, B. M., Chipperfield, M. P., Untch, A., Morcrette, J.-J., Rap, A., and Simmons, A. J.: On the uses of a new linear scheme for stratospheric methane in global models: water source, transport tracer and radiative forcing, Atmos. Chem. Phys., 13, 9641-9660, doi:10.5194/acp-13-9641-2013, 2013.

Morcrette, J.-J., Boucher, O., Jones, L., Salmond, D. , Bechtold, P., Beljaars, A., Benedetti, A., Bonet, A., Kaiser, J. W., Razinger, M., Schulz, M. , Serrar, S. , Simmons, A. J., Sofiev, M., Suttie, M., Tompkins, A. M. and Untch, A.: Aerosol analysis and forecast in the ECMWF Integrated Forecast System. Part I: Forward modelling, J. Geophys. Res., 2009.

Michou M., P. Laville, D. Serça, A. Fotiadi, P. Bouchou and V.-H. Peuch, Measured and modeled dry deposition velocities over the ESCOMPTE area, Atmos. Res., 74 (1-4), 89-116, 2004.

Muncaster, R., Bourqui, M. S., Chabrillat, S., Viscardy, S., Melo, S., and Charbonneau, P.: A simple framework for modelling the photochemical response to solar spectral irradiance variability in the stratosphere, Atmos. Chem. Phys., 12, 7707-7724, doi:10.5194/acp-12-7707-2012, 2012.

Pausata, F. S. R., Pozzoli, L., Vignati, E., and Dentener, F. J.: North Atlantic Oscillation and tropospheric ozone variability in Europe: model analysis and measurements intercomparison, Atmos. Chem. Phys., 12, 6357-6376, doi:10.5194/acp-12-6357-2012, 2012.

Platt, U. and Stutz, J.: Differential Optical Absorption Spectroscopy, Physics of Earth and Space Environments, Berlin: Springer, available at: http://www.springerlink.com/content/978-3-540-21193-8 (last access: February 2016), 2008.

Read, W., Lambert, A., Bacmeister, J., Cofield, R., Christensen, L., Cuddy, D., Daffer, W., Drouin, B., Fetzer, E., Froidevaux, L., et al.: Aura Microwave Limb Sounder upper tropospheric and lower stratospheric H2O and relative humidity with respect to ice validation, Journal of Geophysical Research: Atmospheres, 112, 2007.

Robichaud, A., Ménard, R., Chabrillat, S., de Grandpré, J., Rochon, Y. J., Yang, Y. and Charette, C : Impact of energetic particle precipitation on stratospheric polar constituents: an assessment using monitoring and assimilation of operational MIPAS data, Atmos. Chem. Phys, 10, 1739-1757, doi:10.5194/acp-10-1739-2010, 2010.

Qu, Z., Gschwind, B., Lefevre, M., and Wald, L.: Improving HelioClim-3 estimates of surface solar irradiance using the McClear clear-sky model and recent advances in atmosphere composition, Atmos. Meas. Tech., 7, 3927-3933, doi:10.5194/amt-7-3927-2014, 2014.

Raspollini, P., Carli, B., Carlotti, M., Ceccherini, S., Dehn, A., Dinelli, B. M., Dudhia, A., Flaud, J.-M., López-Puertas, M., Niro, F., Reme- dios, J. J., Ridolfi, M., Sembhi, H., Sgheri, L., and von Clarmann, T.: Ten years of MIPAS measurements with ESA Level 2 processor V6 – Part 1: Retrieval algorithm and diagnostics of the products, Atmos. Meas. Tech., 6, 2419–2439, doi:10.5194/amt-6-2419-2013, http://www.atmos-meas-tech.net/6/2419/2013/, 2013.

Richter, A., Burrows, J. P., Nüß, H., Granier, C, Niemeier, U.: Increase in tropospheric nitrogen dioxide over China observed from space, Nature, 437, 129-132, doi: 10.1038/nature04092, 2005.

Sander, S.P., et al., Chemical Kinetics and Photochemical Data for Use in Stratospheric Modeling. Supplement to Evaluation 12: Update of Key Reactions, Evaluation Number 13, JPL Publication 00-03, Jet Propulsion Laboratory, Pasadena, 2000.

Sander, S.P., et al., Chemical Kinetics and Photochemical Data for Use in Atmospheric Studies. Evaluation Number 15. JPL Publication 06-2, Pasadena, 2006.

Sander, S. P., Abbatt, J. R., Burkholder, J. B., Friedl, R. R., Golden, D. M., Huie, R. E., Kolb, C. E., Kurylo, G., Moortgat, K., Orkin, V. L. and Wine, P. H.: Chemical kinetics and Photochemical Data for Use in Atmospheric studies, Evaluation No.17, JPL Publication 10-6, Jet Propulsion Laboratory, Pasadena, 2011.

Sandu, A. and Sander, R.: Technical note: Simulating chemical systems in Fortran90 and Matlab with the Kinetic PreProcessor KPP-2.1, Atmos. Chem. Phys., 6, 187-195, doi:10.5194/acp-6-187-2006, 2006.

Scaife, A., Spangehl, T., Fereday, D., Cubasch, U., Langematz, U., Akiyoshi, H., Bekki, S., Braesicke, P., Butchart, N., Chipperfield, M., Gettelman, A., Hardiman, S., Rozanov, M. M. E., and Shepherd, T.: Climate change projections and stratosphere-troposphere interaction, Climate Dyn., 38, 2089–2097, doi:10.1007/s00382-011-1080-7, 2012.

Solomon, S., Rosenlof, K. H., Portmann, R.W., Daniel, J. S., Davis, S. M., Sanford, T. J., and Plattner, G.-K.: Contributions of stratospheric water vapor to decadal changes in the rate of global warming, Science, 327, 1219–1223, 2010

Stevenson, D. S. and Dentener, F. J. and Schultz, M. G. and Ellingsen, K. and van Noije, T. P. C. and Wild, O. and Zeng, G. and Amann, M. and Atherton, C. S. and Bell, N. and Bergmann, D. J. and Bey, I. and Butler, T. and Cofala, J. and

Collins, W. J. and Derwent, R. G. and Doherty, R. M. and Drevet, J. and Eskes, H. J. and Fiore, A. M. and Gauss, M. and Hauglustaine, D. A. and Horowitz, L. W. and Isaksen, I. S. A. and Krol, M. C. and Lamarque, J.-F. and Lawrence, M. G. and Montanaro, V. and Müller, J.-F. and Pitari, G. and Prather, M. J. and Pyle, J. A. and Rast, S. and Rodriguez, J. M. and Sanderson, M. G. and Savage, N. H. and Shindell, D. T. and Strahan, S. E. and Sudo, K. and Szopa, S. .: Multimodel ensemble simulations of present-day and near-future tropospheric ozone, J. Geophys. Res., 111, D08301, doi:10.1029/2005JD006338, 2006.

Strong, K., Wolff, M. A., Kerzenmacher, T. E., Walker, K. A., Bernath, P. F., Blumenstock, T., Boone, C., Catoire, V., Coffey, M., De Mazière, M., Demoulin, P., Duchatelet, P., Dupuy, E., Hannigan, J., Höpfner, M., Glatthor, N., Griffith, D. W. T., Jin, J. J., Jones, N., Jucks, K., Kuellmann, H., Kuttippurath, J., Lambert, A., Mahieu, E., McConnell, J. C., Mellqvist, J., Mikuteit, S., Murtagh, D. P., Notholt, J., Piccolo, C., Raspollini, P., Ridolfi, M., Robert, C., Schneider, M., Schrems, O., Semeniuk, K., Senten, C., Stiller, G. P., Strandberg, A., Taylor, J., Tétard, C., Toohey, M., Urban, J., Warneke, T., and Wood, S.: Validation of ACE-FTS N2O measurements, Atmos. Chem. Phys., 8, 4759–4786, doi:10.5194/acp-8-4759-2008, http://www.atmos-chem-phys.net/8/4759/2008/, 2008.

SPARC CCMVal Report on the Evaluation of Chemistry-Climate Models, V. Eyring, T. G. Shepherd, D. W. Waugh (Eds.), SPARC Report No. 5, WCRP-X, WMO/TD-No. X, 2010., http://www.sparc-climate.org/publications/, 2010.

Talagrand, O. and Courtier, P.: Variational assimilation of meteorological observations with the adjoint vorticity equation, I, Theory, Q. J. Roy. Meteor. Soc., 23, 1311–1328, 1987.

Theys, N., Van Roozendael, M., Errera, Q., Hendrick, F., Daerden, F., Chabrillat, S., Dorf, M., Pfeilsticker, K., Rozanov, A., Lotz, W., Burrows, J. P., Lambert, J.-C., Goutail, F., Roscoe, H. K. and De Mazière, M.: A global stratospheric bromine monoxide climatology based on the BASCOE chemical transport model, Atmos. Chem. Phys., 9, 831-848, doi: 10.5194/acp-9-831-2009, 2009.

Thornton, H. E., Jackson, D. R., Bekki, S., Bormann, N., Errera, Q., Geer, A. J., Lahoz, W. L., and Rhalmili, S., The ASSET intercomparison of stratosphere and lower mesosphere humidity analyses, Atmos. Chem. Phys., 9 995-116 (2009).

Thuburn, J., and G. Craig, GCM tests of theories for the height of the tropopause, J. Atmos. Sci., 54, 869–882, 1997.

van der A, R. J., Allaart, M. A. F., and Eskes, H. J.: Extended and refined multi sensor reanalysis of total ozone for the period 1970–2012, Atmos. Meas. Tech., 8, 3021-3035, doi:10.5194/amt-8-3021-2015, 2015.

Viscardy, S., Errera, Q., Christophe, Y., Chabrillat, S. and Lambert, J. -C.: Evaluation of Ozone Analyses From UARS MLS Assimilation by BASCOE Between 1992 and 1997, IEEE J-STARS, 3, 190-202, doi:10.1109/JSTARS.2010.2040463, 2010.

von Glasow, R. and Crutzen, P. J.: Tropospheric halogen chemistry, in: The Atmosphere (ed. R. F. Keeling), Vol. 4 Treatise on Geochemistry (eds. H. D. Holland and K. K. Turekian), Elsevier-Pergamon, Oxford, 2007.

Wang, D. Y., Höpfner, M., Blom, C. E., Ward, W. E., Fischer, H., Blumenstock, T., Hase, F., Keim, C., Liu, G. Y., Mikuteit, S., Oelhaf, H., Wetzel, G., Cortesi, U., Mencaraglia, F., Bianchini, G., Redaelli, G., Pirre, M., Catoire, V., Huret, N., Vigouroux, C., De Mazière, M., Mahieu, E., Demoulin, P., Wood, S., Smale, D., Jones, N., Nakajima, H., Sugita, T.,

Urban, J., Murtagh, D., Boone, C. D., Bernath, P. F., Walker, K. A., Kuttippurath, J., Kleinböhl, A., Toon, G., and Piccolo, C.: Validation of MIPAS HNO3 operational data, Atmos. Chem. Phys., 7, 4905-4934, doi:10.5194/acp-7-4905-2007, 2007.

Wesely, M.L.: Parameterization of Surface Resistances to Gaseous Dry Deposition in Regional-Scale Numerical Models. Atmos. Environ., 23, 1293-1304, 1989.

Wetzel, G., Bracher, A., Funke, B., Goutail, F., Hendrick, F., Lambert, J.-C., Mikuteit, S., Piccolo, C., Pirre, M., Bazureau, A., Belotti, C., Blumenstock, T., De Mazière, M., Fischer, H., Huret, N., Ionov, D., López-Puertas, M., Maucher, G., Oelhaf, H., Pommereau, J.-P., Ruhnke, R., Sinnhuber, M., Stiller, G., Van Roozendael, M., and Zhang, G.: Validation of MIPAS-ENVISAT NO2 operational data, Atmos. Chem. Phys., 7, 3261-3284, doi:10.5194/acp-7-3261-2007, 2007.

Williams, J. E., Strunk, A., Huijnen, V., and van Weele, M.: The application of the Modified Band Approach for the calculation of on-line photodissociation rate constants in TM5: implications for oxidative capacity, Geosci. Model Dev., 5, 15-35, doi:10.5194/gmd-5-15-2012, 2012.

Williams, J. E., van Velthoven, P. F. J., and Brenninkmeijer, C. A. M.: Quantifying the uncertainty in simulating global tropospheric composition due to the variability in global emission estimates of Biogenic Volatile Organic 2857-2013, 2013.

Wittrock, F., A. Richter, H. Oetjen, J. P. Burrows, M. Kanakidou, S. Myriokefalitakis, R. Volkamer, S. Beirle, U. Platt, and T. Wagner, Simultaneous global observations of glyoxal and formaldehyde from space, Geophys. Res. Lett., 33, L16804, doi:10.1029/2006GL026310, 2006Compounds, Atmos. Chem. Phys., 13, 2857-2891, doi:10.5194/acp-13-2857-2013, 2013.

World Meteorological Organization (WMO), Meteorology A Three-Dimensional Science: Second Session of the Commission for Aerology, WMO Bulletin IV(4), WMO, Geneva, 134–138, 1957.

Yarwood, G., Rao, S., Yocke, M., and Whitten, G.: Updates to the carbon bond chemical mechanism: CB05. Final report to the US EPA, EPA Report Number: RT-0400675, available at: www.camx.com, last access: 16 July 2015, 2005.

Geosci. Model Dev. Discuss., doi:10.5194/gmd-2016-40, 2016
Manuscript under review for journal Geosci. Model Dev.
Published: 7 March 2016

Geoscientific Model Development Discussions

Table 1. Trace gases relevant for the stratosphere which are constrained at the surface. The constant surface volume mixing ratios are also given.

N_2O	CFC11	CFC12	CFC113	CFC114	CCl_4	CH_3CCl_3
3.22E-7	2.59E-10	5.37E-10	7.93E-11	4.25E-12	1.02E-10	4.53E-11
HCFC22	HA1301	HA1211	CH_3Br	$CHBR_3$	CH_3Cl	CO_2
1.70E-10	3.30E-12	4.62E-12	9.08E-12	1.17E-12	5.44E-10	3.80E-4

Table 2. Number of tracers, reactions (gas-phase / heterogeneous and photolytic), and computational expenses of a one-month run on T255L60 in terms of system billing units (SBU) for various C-IFS model versions.

	C-IFS-T	C-IFS-S	C-IFS-TS
No. tracers	55	59	99
No. reactions (gas / het / photo)	93/3/18	142/9/52	93/3/18 *or* 142/9/52
SBU	2075	2500	3076

Table 3. Parameterization of photolysis rates for troposphere (CB05-based) and stratosphere (BASCOE-based)

	Troposphere (Williams et al., 2012)	**Stratosphere** (Errera and Fonteyn, 2001)
No. J-rates	18	52
Method	2-stream online solver, 204<λ<705nm	Lookup table approach, 116<λ<705nm
Dependencies	O_3 overhead, pressure, solar zenith angle, cloud, aerosol, surface albedo, temperature	O_3 overhead, pressure, solar zenith angle
terminator treatment	J>0 for sza<85°	J>0 for sza<96°, Chapman approximation

Geosci. Model Dev. Discuss., doi:10.5194/gmd-2016-40, 2016
Manuscript under review for journal Geosci. Model Dev.
Published: 7 March 2016

Geoscientific Model Development Discussions

Table 4. Selection of photolytic reactions that are merged between troposphere and stratosphere. The reaction product O_2 is not shown.

Name	**reaction (stratosphere)**	**reaction products (troposphere)[a]**
J O3	$O_3 + h\nu \rightarrow O^1D$	
J NO2	$NO_2 + h\nu \rightarrow NO + O$	$NO + O_3$
J H2O2	$H_2O_2 + h\nu \rightarrow 2OH$	
J HNO3	$HNO_3 + h\nu \rightarrow OH + NO_2$	
J HO2NO2	$HO_2NO_2 + h\nu \rightarrow HO_2 + NO_2$	
J N2O5	$N_2O_5 + h\nu \rightarrow NO_2 + NO_3$	
J CH2O-a	$CH_2O + h\nu \rightarrow HCO + H$	$CO + 2HO_2$
JCH2O-b	$CH_2O + h\nu \rightarrow CO + H_2$	CO
J NO3-a	$NO_3 + h\nu \rightarrow NO_2 + O$	$NO_2 + O_3$
J NO3-b	$NO_3 + h\nu \rightarrow NO$	
J O2	$O_2 + h\nu \rightarrow 2O$	
J CH3OOH	$CH_3OOH + h\nu \rightarrow CH_3O + OH$	$CH_2O + HO_2 + OH$

[a] Only specified in case this is different from the stratospheric reaction.

Geosci. Model Dev. Discuss., doi:10.5194/gmd-2016-40, 2016
Manuscript under review for journal Geosci. Model Dev.
Published: 7 March 2016

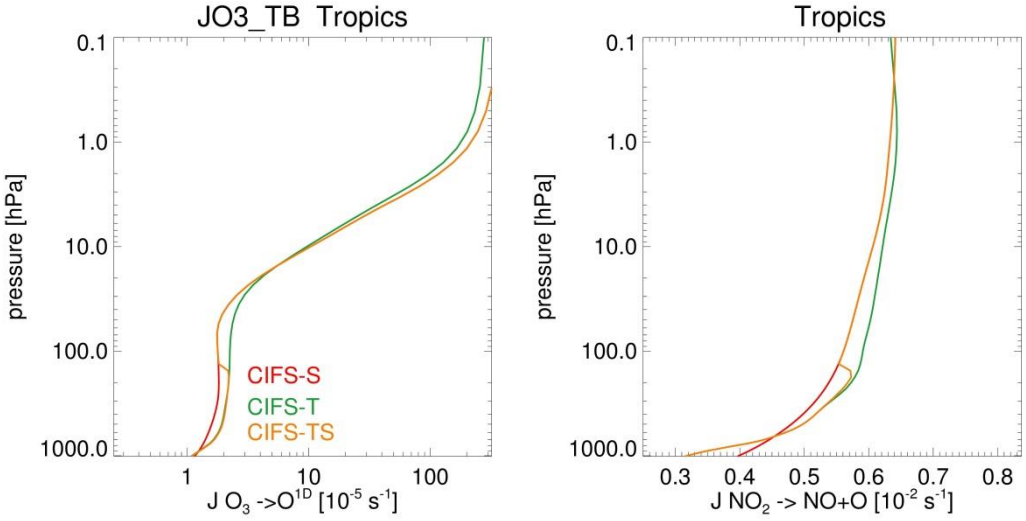

Figure 1. Illustration of the merging procedure for photolysis rates between the tropospheric and stratospheric parameterizations for the reaction $O_3 \rightarrow O^1D$ (left) and $NO_2 \rightarrow NO+O$ (right) as zonally averaged over the tropics for 1 April 2008.

Geosci. Model Dev. Discuss., doi:10.5194/gmd-2016-40, 2016
Manuscript under review for journal Geosci. Model Dev.
Published: 7 March 2016

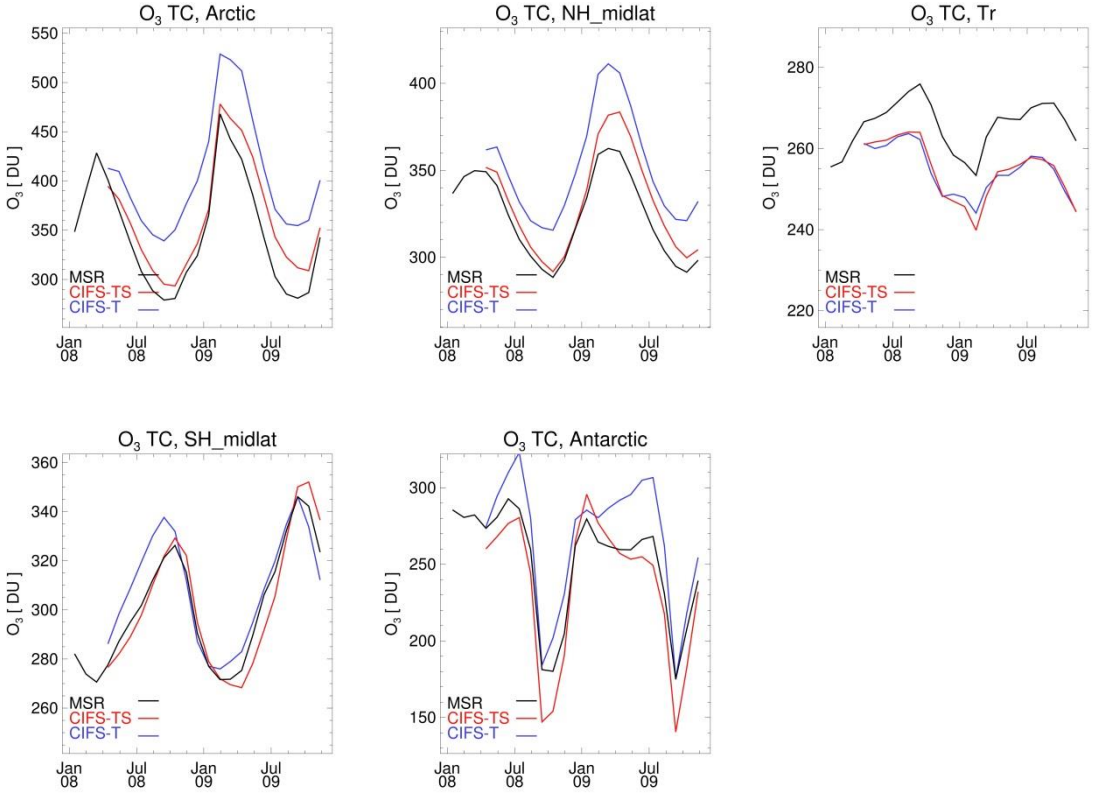

Figure 2. Evaluation of monthly mean O_3 total columns in Dobson Units against the Multi-Sensor Reanalysis for the Arctic (90°N-70°N), Northern mid-latitudes (60°N-30°N), tropics (30°N-30°S), Southern Hemisphere mid-latitudes (30°S-60°S) and Antarctica (70°S-90°S).

Geosci. Model Dev. Discuss., doi:10.5194/gmd-2016-40, 2016
Manuscript under review for journal Geosci. Model Dev.
Published: 7 March 2016

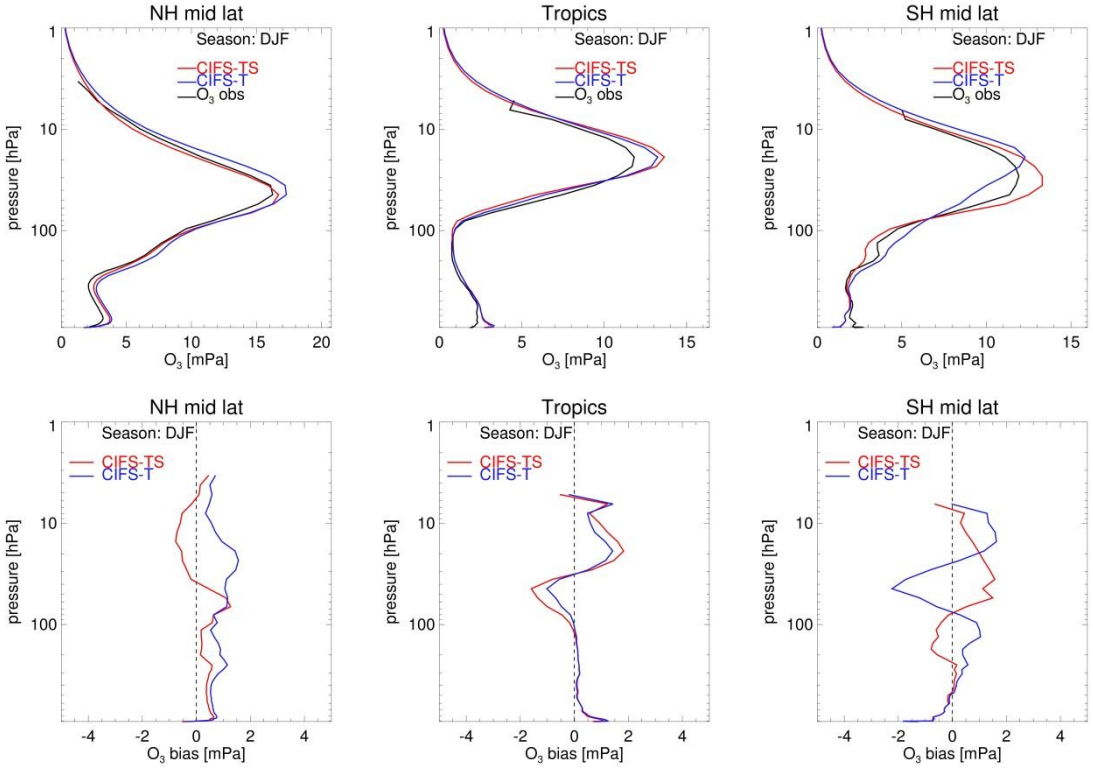

Figure 3. Top row: evaluation of ozone in units mPa against WOUDC sondes over NH mid-latitudes (60°N-30°N, left), tropics (30°N-30°S, middle) and SH mid-latitudes(30°S-60°S, right) for December-January-February 2009 in units mPa. Black: WOUDC observations, red: C-IFS-TS, blue: C-IFS-T. Bottom row: corresponding mean biases.

Geosci. Model Dev. Discuss., doi:10.5194/gmd-2016-40, 2016
Manuscript under review for journal Geosci. Model Dev.
Published: 7 March 2016

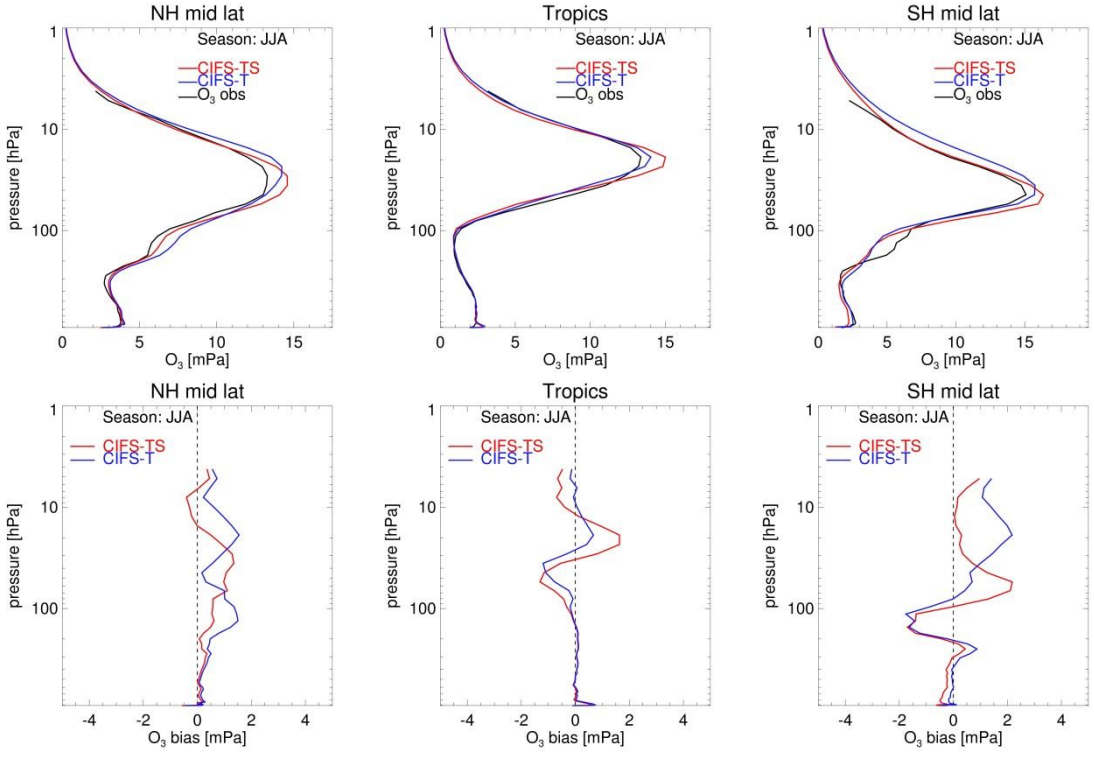

Figure 4. Same as Fig. 3, but for June-July-August 2009.

Geosci. Model Dev. Discuss., doi:10.5194/gmd-2016-40, 2016
Manuscript under review for journal Geosci. Model Dev.
Published: 7 March 2016

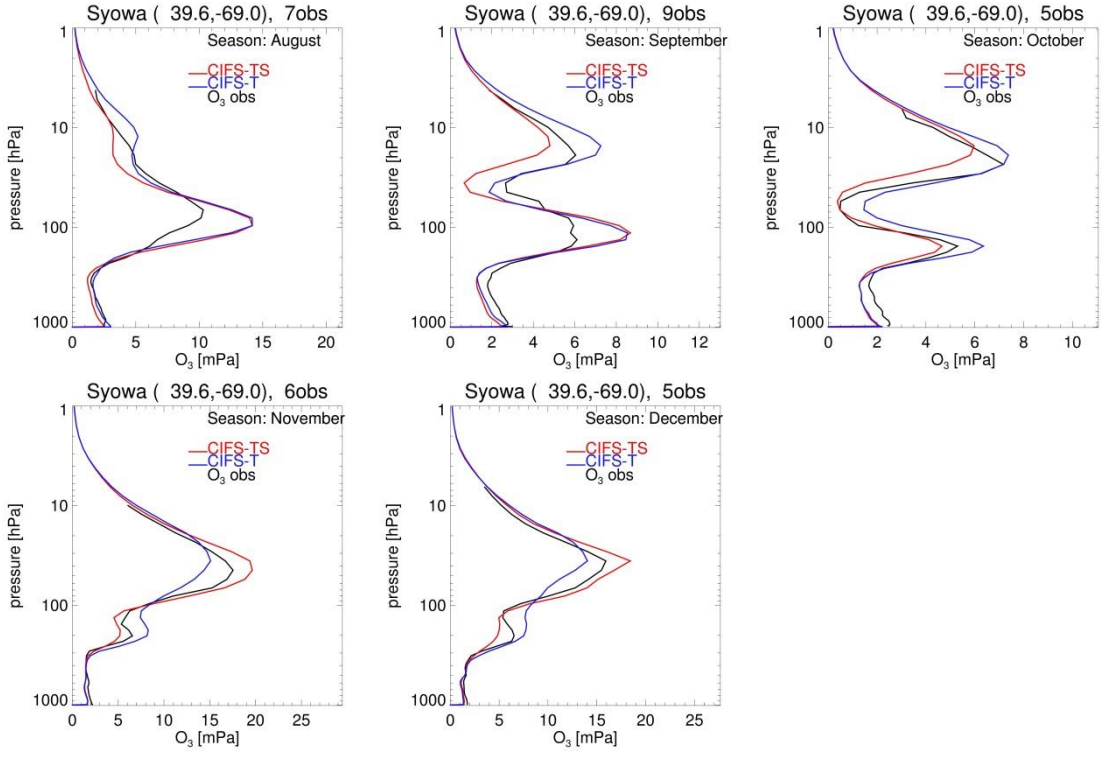

Figure 5. Evaluation of ozone in units mPa against WOUDC ozone sondes at Syowa station during August-December 2009. Black: ozone sonde, Red: C-IFS-TS, blue: C-IFS-T.

Geosci. Model Dev. Discuss., doi:10.5194/gmd-2016-40, 2016
Manuscript under review for journal Geosci. Model Dev.
Published: 7 March 2016

Geoscientific Model Development Discussions

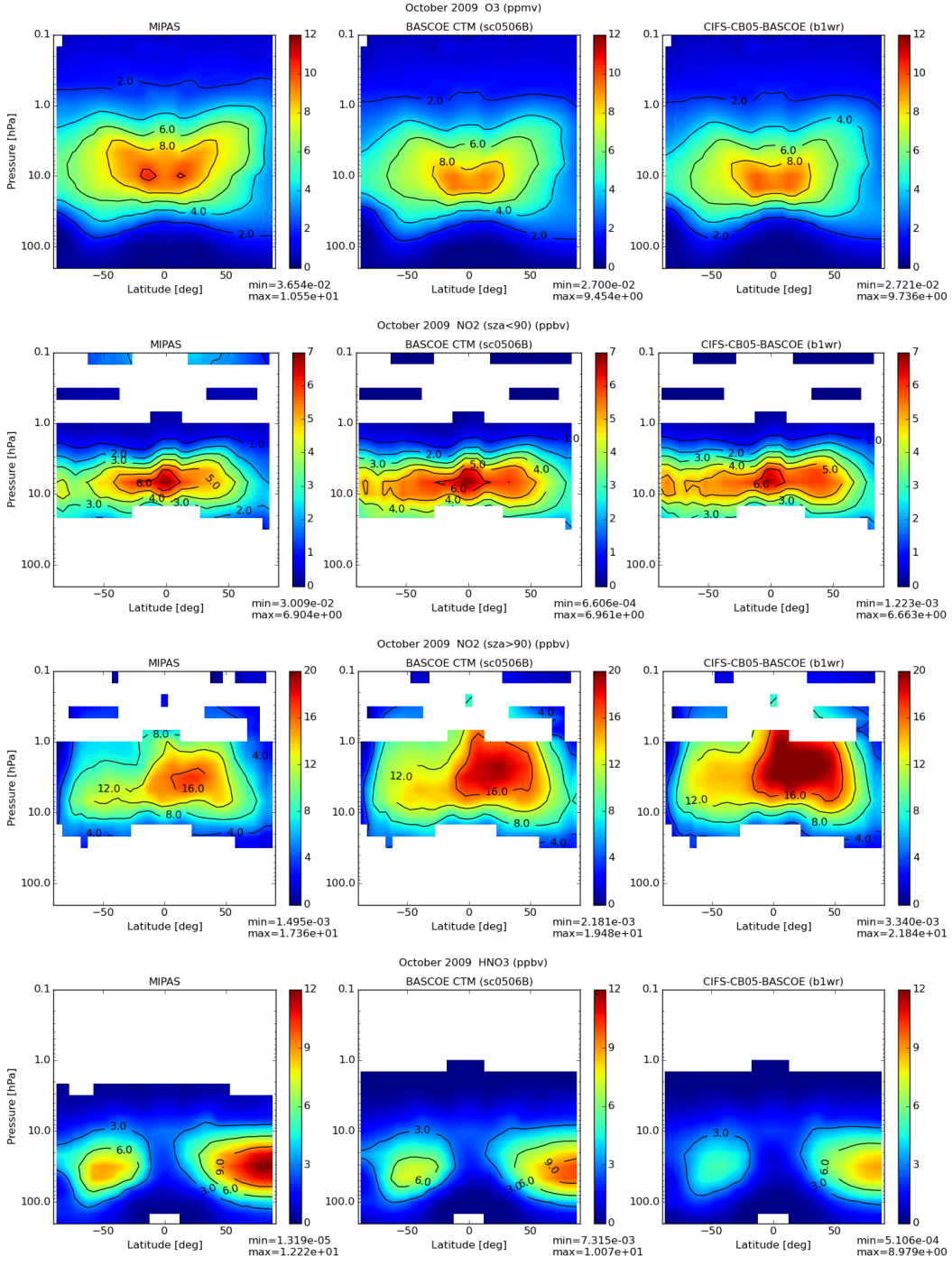

Figure 6. Zonal mean stratospheric O_3 (top row, units ppmv), daytime NO_2 (second row) and night-time NO_2 (third row) and HNO_3 (bottom row, all in units ppbv) for October 2009 using MIPAS observations (left) and co-located output of BASCOE-CTM (middle) and C-IFS-TS (right).

Geosci. Model Dev. Discuss., doi:10.5194/gmd-2016-40, 2016
Manuscript under review for journal Geosci. Model Dev.
Published: 7 March 2016

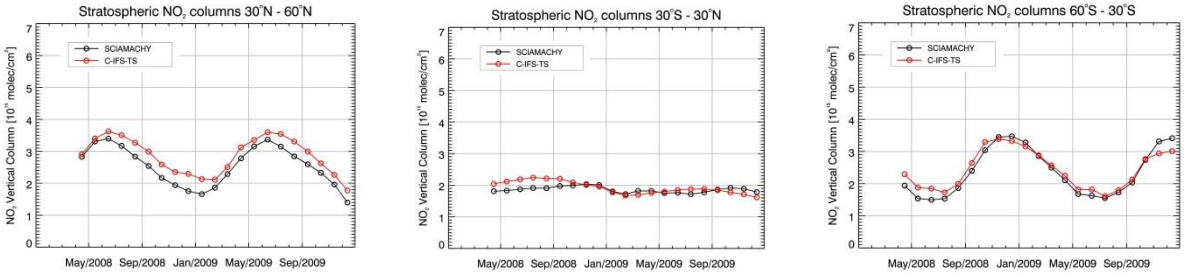

Figure 7. Time series of stratospheric NO_2 for April 2008 – Dec 2009 of C-IFS-TS against SCIAMACHY, in units 10^{15} molec cm^{-2} for NH mid-latitudes (left), tropics (middle) and SH mid-latitudes (right).

Geosci. Model Dev. Discuss., doi:10.5194/gmd-2016-40, 2016
Manuscript under review for journal Geosci. Model Dev.
Published: 7 March 2016

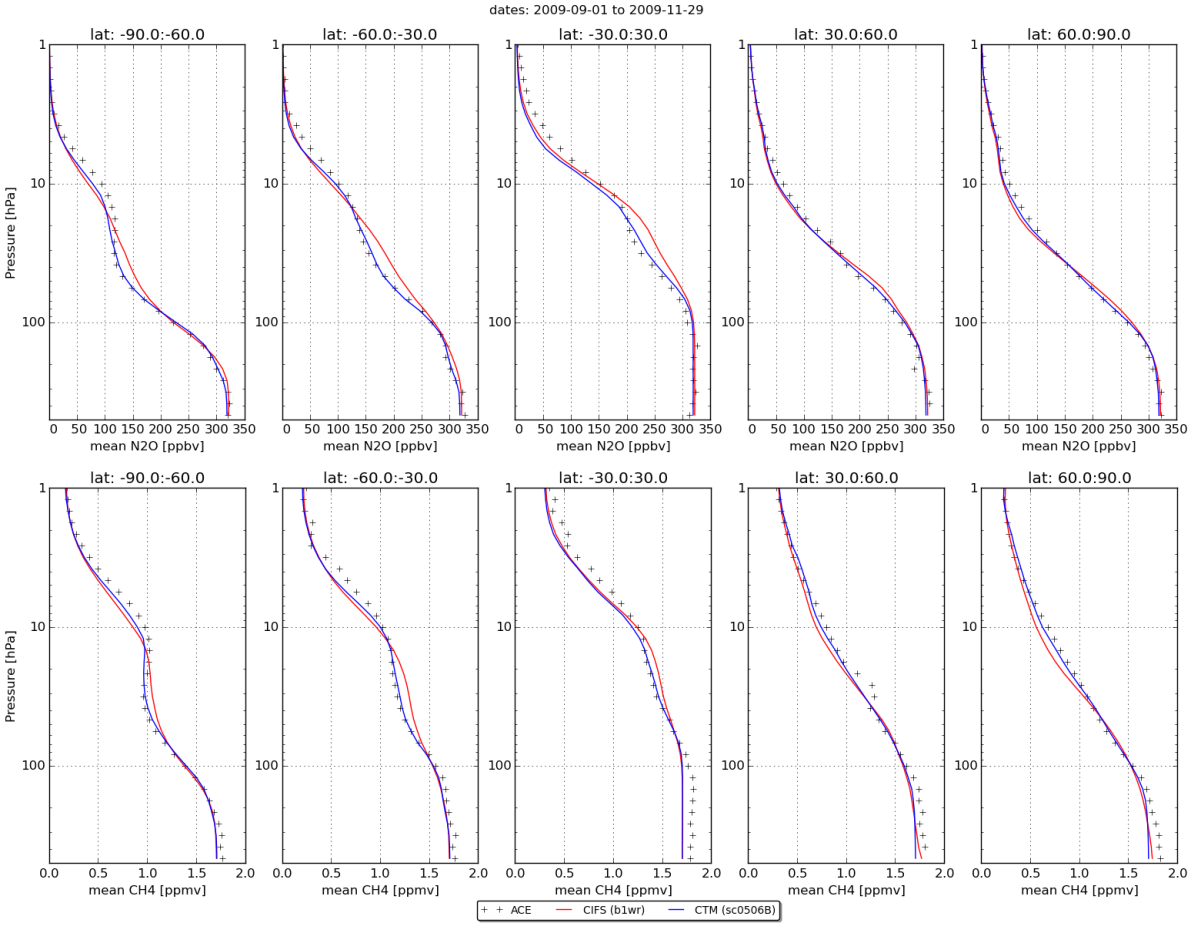

Figure 8. Zonal mean profiles of stratospheric N_2O (top) and CH_4 (bottom) for September-October-November 2009 using ACE-FTS observations (black symbols) and co-located output of BASCOE-CTM (blue lines) and C-IFS-TS (red lines). The zonal means are shown separately on five columns corresponding to the latitude bands 90°S-60°S, 60°S-30°S, 30°S-30°N, 30°N-60°N and 60°N-90°N, respectively.

Geosci. Model Dev. Discuss., doi:10.5194/gmd-2016-40, 2016
Manuscript under review for journal Geosci. Model Dev.
Published: 7 March 2016

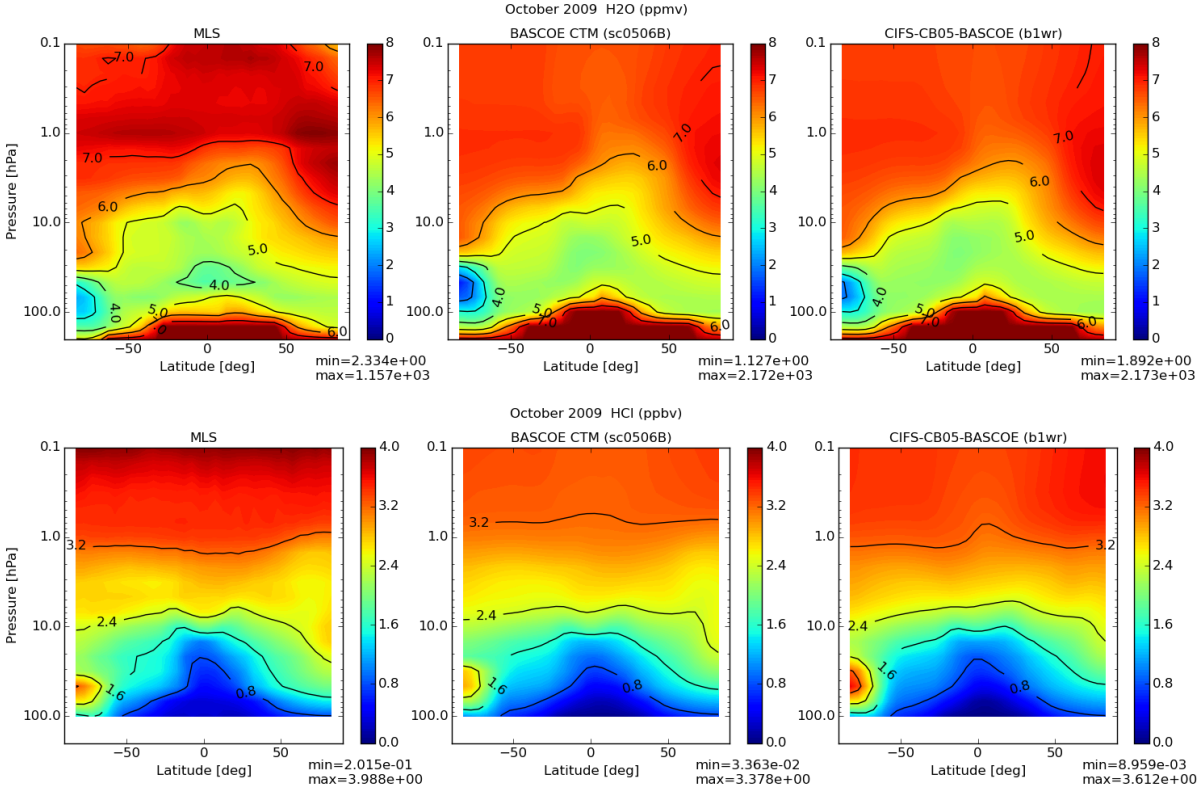

Figure 9. Zonal mean stratospheric H_2O (top, units ppmv) and HCl (bottom, units ppbv) for October 2009 using Aura/MLS observations (left) and co-located output of BASCOE-CTM (middle) and C-IFS-TS (right).